Available online at www.sciencedirect.com
ScienceDirect
Journal of the European Ceramic Society 32 (2012) 133–139
www.elsevier.com/locate/jeurceramsoc

Dielectric and piezoelectric behaviors of NBT-$BT_{0.05}$ processed by sol–gel method

Marin Cernea [a,d,*], Bogdan S. Vasile [b,d], Claudio Capiani [b,d], Anghel Ioncea [c,d], Carmen Galassi [b,d]

[a] National Institute of Materials Physics, P.O. Box MG-7, Bucharest-Magurele 077125, Romania
[b] University Politehnica of Bucharest, 060042, Romania
[c] METAV-R&D S. A., P.O. 22, Bucharest, Romania
[d] National Research Council - Institute of Science and Technology for Ceramics, Via Granarolo 64, I-48018 Faenza, Italy

Received 12 April 2011; received in revised form 20 July 2011; accepted 25 July 2011
Available online 19 August 2011

Abstract

$(Na_{0.5}Bi_{0.5})TiO_3$ doped with 5 mol% $BaTiO_3$ (NBT-$BT_{0.05}$) nanopowder was prepared by sol–gel method. Structural and microstructural investigations revealed a powder crystallized in the $Na_{0.5}Bi_{0.5}TiO_3$ rhombohedral phase form. Ceramics processed from this powder show good dielectric ($\varepsilon_r = 3940$ and $\tan\delta = 0.016$) and piezoelectric characteristics ($d_{33} = 77$ pC/N, $k_p = 0.091$, $\varepsilon_{33}^T = 1080$ and $Q_m = 197.5$). The as-obtained NBT-$BT_{0.05}$ ceramic appears effective for piezoelectric resonator and high power applications.

Keywords: A. Sol–gel processes; C. Dielectric properties; C. Piezoelectric properties; D. $BaTiO_3$ and titanates

1. Introduction

$Na_{0.5}Bi_{0.5}TiO_3$ ceramic and its variations is a promising piezoelectric material without lead. This material is now intensively investigated in the aim of the improvement in piezoelectric characteristics. Various methods are used to synthesis doped/undoped $Na_{0.5}Bi_{0.5}TiO_3$ and its solid solutions with microstructural features required for engineering these properties.[1–7] Grain size is an important microstructural characteristic that affects piezoelectric properties. Although the piezoelectric properties are expected to degrade with smaller grain size, the relative permittivity increases. Moreover, finer grain piezoelectric offers two main advantages; higher mechanical strength and improved dielectric strength, if the piezoelectric properties could be preserved. Recently, considerable research efforts have been devoted to the preparation of NBT-based ceramics by various wet chemical methods, such as citrate method,[1,8] emulsion method,[9] hydrothermal process,[10] stearic acid gel route[11] and sol gel techniques.[2,3,6,12,13] It was found that NBT-based ceramics made from powders synthesized by alternative methods exhibit improved sinterability, poling process and piezoelectric properties.[13] Moreover, to improve the poling capacity of NBT, the partial substitution of A-site ions $(Na_{0.5}Bi_{0.5})^{2+}$ by Ba^{2+}, $(K_{0.5}Bi_{0.5})^{2+}$ and others[1,6,9] is used. Among the solid solutions that have been developed so far, $(Na_{0.5}Bi_{0.5})_{1-x}Ba_xTiO_3$ (NBT-BT_x) system has attracted considerable attention, because of the existence of a rhombohedral–tetragonal morphotropic phase boundary (MPB) near $x = 0.06$–0.08, where the materials show significantly enhanced piezoelectric properties and reduced coercive field.[2,14–16] In this paper, we study the influence of the sol–gel synthesis method and highlight ($BaTiO_3$) concentration that located NBT-$BT_{0.05}$ ceramic at MPB region low limit, on the structure and electrical properties of this ceramic.

2. Experimental procedure

Precursor sol of $0.95[(Na_{0.5}Bi_{0.5})TiO_3]$–$0.05[BaTiO_3]$ (NBT-$BT_{0.05}$) was prepared by sol–gel technique. The detailed sol–gel procedure was published in a previous paper.[12] Reagent-grade sodium acetate [$Na(CH_3COO)$], bismuth (III) acetate [$Bi(CH_3COO)_3$], barium acetate [$Ba(CH_3COO)_2$] and titanium (IV) isopropoxide, 97% solution in 2-propanol [$Ti\{OCH(CH_3)_2\}_4$] were used as starting materials and, water

* Corresponding author. Tel.: +40 21 369 01 70x130; fax: +40 21 369 01 77.
E-mail address: mcernea@infim.ro (M. Cernea).

0955-2219/$ – see front matter © 2011 Elsevier Ltd. All rights reserved.
doi:10.1016/j.jeurceramsoc.2011.07.038

and acetic acid as solvents for the preparation of NBT-$BT_{0.05}$ precursor solution.

The gel was investigated by thermal analyses, scanning electronic microscopy (SEM), transmission electronic microscopy (TEM), X-ray diffraction (XRD) and Raman spectroscopy. The thermogravimetric analysis (TG) and differential thermal analysis (DTA) were recorded by using a TGA Instrument (model Pyris Diamond), Perkin Elmer Instruments. The sample was measured in an open cylindrical alumina crucible and the experiment conducted in synthetic air (80% N_2/20% O_2) at a flow rate of 16 ml/min. The temperature was calibrated with bismuth, aluminum and silver, temperature range of the experiments was between 150 and 1300 °C with a heating rate of 10 °C/min. The sample mass was around 37 mg. The microstructure of the samples was investigated using a FEI Quanta Inspect F with EDAX scanning electron microscope and, a Tecnai^{TM} G^2 F30 S-TWIN transmission electron microscope with a line resolution of 1 Å, in high resolution transmission electron microscopy (HR-TEM) mode and selected area electron diffraction (SAED). Raman spectra were recorded at room temperature in a backscattering geometry under excitation wavelength of 1064 nm using a spectrophotometer FT Raman Bruker RFS 100. The Raman spectrum was recorded in the range 100–1000 cm^{-1} using for excitation, the 1064 nm line of a laser. The structure of the NBT-$BT_{0.05}$ precursor powders was characterized by X-ray diffraction technique using a Bruker-AXS tip D8 ADVANCE diffractometer. For powder diffraction, Cu$K\alpha$1 radiation (wavelength 1.5406 Å), LiF crystal monochromator and Bragg-Brentano diffraction geometry were used. The data were acquired at 25 °C with a step-scan interval of 0.020° and a step time of 10 s. The electrical measurements were carried out in the metal–ferroelectric–metal (MFM) configuration, where the electrodes M consist of silver paste. Samples for piezoelectric measurements were poled under applied fields of 3 kV/mm, at 120 °C, 40 min. Then, another 50 min when the temperature decreases up to the room temperature. Piezoelectric properties were measured by a resonance–antiresonance method on the basis of IEEE 176-1987 standards, using an impedance analyzer (HP 4194A). The electromechanical coupling factor (k_{33}), was calculated from the resonance and antiresonance frequencies. The free permittivity (ε_{ii}^{T}), was determined from the capacitance at 1 kHz of the poled specimen. The elastic constants (S_{jj}^{E}), was calculated from the frequency constant (N_{ij}), and the measured density (ρ_0) by the relation of $S_{11}^{E} = 10^9/(\pi^2 N p^2 \rho_0)$. Finally, the piezoelectric constants (d_{ij}), was calculated from the k_{ij}, ε_{ii}^{T} and S_{jj}^{E} by the relation of $d_{ij} = k_{ij}(\varepsilon_{ii}^{T} S_{jj}^{E})^{1/2}$, or directly using a d_{33} Meter Sinocera S5865 (d_{33}).

3. Results and discussion

3.1. Thermal analyses

The thermal stability of the precursor-gel of NBT-$BT_{0.05}$ was analysed until 1300 °C by thermogravimetric analysis (TG) and differential thermal analysis (DTA) (Fig. 1).

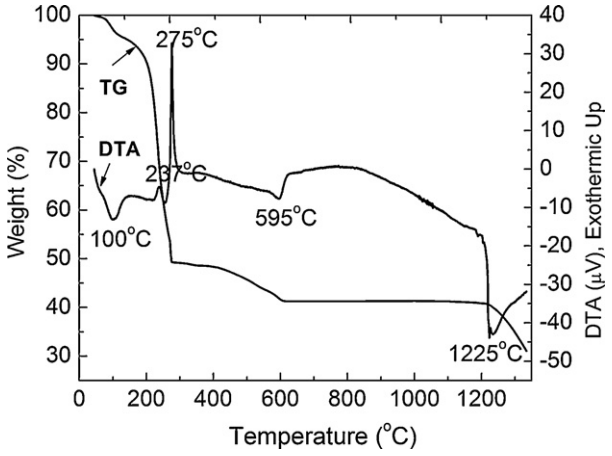

Fig. 1. TG and DTA curves of $BaTiO_3$-doped $Na_{0.5}Bi_{0.5}TiO_3$ precursor gel.

The gel shows a weight loss in two steps; the first stage of precursor decomposition takes place in the temperature range of 25–220 °C and corresponds to the adsorbed water and solvent release; the second stage involves two different steps for the pyrolisis of the organic materials: (1) in the range of 220–275 °C the decomposition occurs at high rate accompanied by a significant weight loss, and (2) in the range of 275–600 °C with slow rate. The second step shows higher weight losses in the 400–600 °C range than in the 275–400 °C. The endothermic peak at 595 °C is due to crystallization of $(Na_{0.5}Bi_{0.5})_{0.95}Ba_{0.05}TiO_3$ solid solution. The weight loss that occurs above 1200 °C corresponds to the partial volatilization of Na and Bi from NBT-$BT_{0.05}$.

3.2. Structure

3.2.1. X-ray diffraction

X-ray diffraction patterns of the of NBT-$BT_{0.05}$ precursor gel, heated at 700 °C and, sintered pellets at 1100, 1150 and 1200 °C, are shown in Fig. 2.

The XRD analyses indicate that when the heating temperature was 700 °C, the gel powder was in the $Na_{0.5}Bi_{0.5}TiO_3$ rhombohedral phase form;[17] on sintering the ceramic pellets at temperatures of 1100, 1150 and 1200 °C, small peaks of a secondary phase appeared. The diffraction peaks of the main phase from NBT-$BT_{0.05}$ ceramic samples can be assigned to the rhombohedral phase of NBT (Fig. 2). According to the reports that one peak near 47° indicates all samples have rhombohedral symmetry structure and a splitting peak near 47° indicates the tetragonality of the samples.[18–20] Fig. 2(b) is the magnification of Fig. 2(a) in the range from 45 to 50°. The feature peak at about 47° does not split in the figure, which indicates that all ceramics have rhombohedral symmetry structure.

3.2.2. Raman spectroscopy

Raman spectroscopy of NBT-$BT_{0.05}$ powder heat-treated at 700 °C was measured at room temperature (Fig. 3).

The spectrum of NBT-$BT_{0.05}$ precursor gel shows peaks at 137, 270, 535 and 812 cm^{-1}, (Fig. 3). For comparison, the A_1(TO) absorption bands of rhombohedral NBT appear

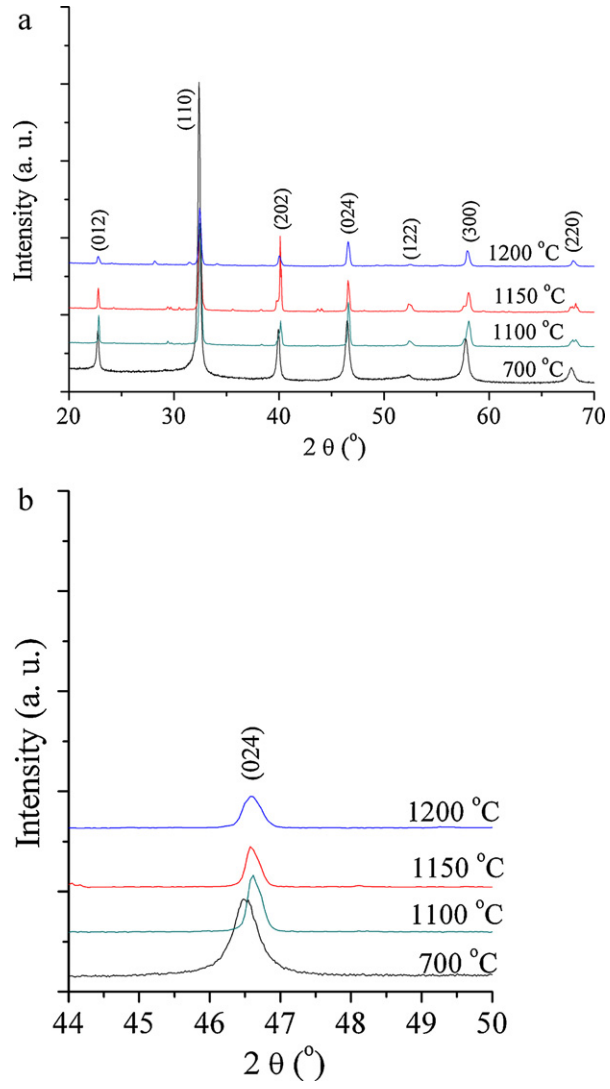

Fig. 2. XRD patterns of NBT-$BT_{0.05}$ precursor gel, heated at 700 °C and, sintered pellets at 1100, 1150 and 1200 °C.

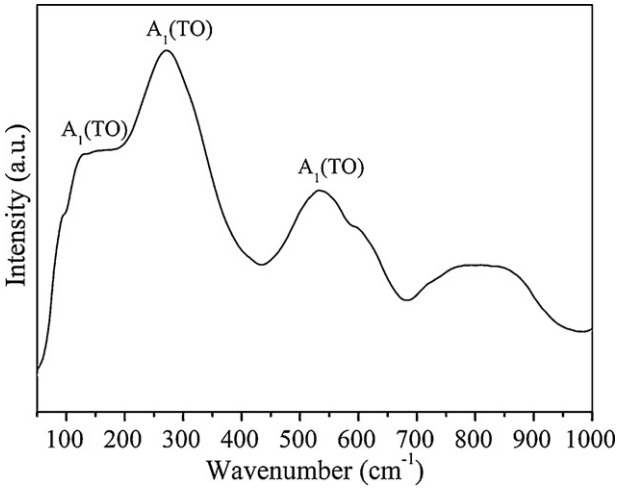

Fig. 3. Raman spectrum of NBT-$BT_{0.05}$ precursor gel heated at 700 °C.

at 130, 269, and 541 cm^{-1} and an E(TO) band appears at 52.5 cm^{-1}.[21,22] Therefore, the Raman spectrum of the NBT-$BT_{0.05}$ powder (Fig. 3) indicates a rhombohedral structure similar to that of NBT. The small shift of NBT-$BT_{0.05}$ peaks can be attributed to the A-site disorder due to doping with $BaTiO_3$. This produces an increase in the lattice parameters explained by higher ionic radii of Ba^{2+} compared to Na^+ and Bi^{3+} ($r_{Ba^{2+}}$ = 0.160 nm; r_{Na^+} = 0.139 nm; $r_{Bi^{3+}}$ = 0.128 nm).[23]

3.3. Microstructure

3.3.1. SEM analysis

The SEM micrographs of $Na_{0.5}Bi_{0.5}TiO_3$ doped with 5 mol% $BaTiO_3$ precursor gel, heated at 600 °C, 2 h in air, is presented in Fig. 4.

As can be seen in Fig. 4, the calcined gel shows a microstructure consisting of fine grains of about 50–60 nm in diameter. The grains are uniform as shape and size. This homogeneity of the powder morphology is characteristic to the powders obtained by sol–gel.

3.3.2. TEM-HRTEM-SAED analyses

The TEM and HRTEM micrographs of NBT-$BT_{0.05}$ precursor gel, heated at 600 °C are shown in Fig. 5(a and b). The TEM bright field image reveals that the powder is composed of polyhedral shaped particles, with an average grain size of approximately 50 nm. The nanopowder also has the tendency to form hard agglomerates, partially sintered.

The HR-TEM image (Fig. 5(b)) shows clear lattice fringes of two polycrystalline nanoparticles of d = 3.88 and 2.74 Å, corresponding to the (0 1 2) and (1 1 0) crystallographic planes of the rhombohedral phase of $Na_{0.5}Bi_{0.5}TiO_3$. Also, the regular succession of the atomic planes indicates that the nanocrystallites are structurally uniform and crystalline with almost no amorphous phase present. The only phase identified from SAED pattern is the rhombohedral one of $Na_{0.5}Bi_{0.5}TiO_3$ (Fig. 5(c)). Both

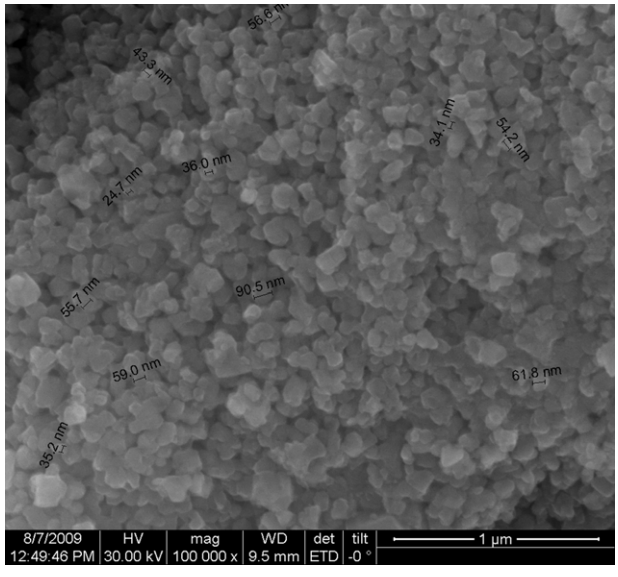

Fig. 4. SEM photomicrographs of NBT-$BT_{0.05}$ precursor gel, heated at 600 °C.

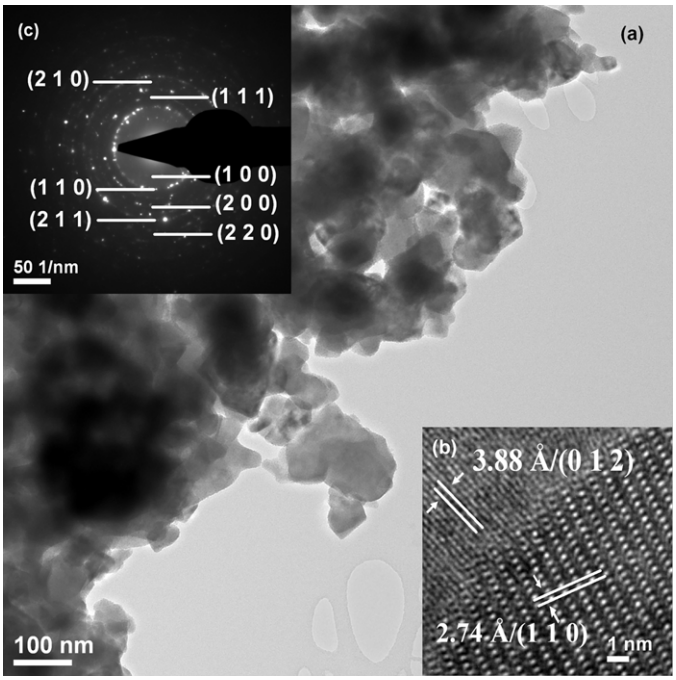

Fig. 5. TEM images of NBT-$BT_{0.05}$ precursor gel, heated at 600 °C (a), corresponding HR-TEM of nanocrystals (b) and SAED image (c).

HR-TEM image and SAED patterns for NBT-$BT_{0.05}$ powder calcined at 600 °C, indicated a rhombohedral $Na_{0.5}Bi_{0.5}TiO_3$ crystallographic phase, in good agreement with XRD analysis (Fig. 2).

3.4. Sintering behaviour and piezoelectric characterization

The ceramic samples were prepared by uniaxial pressing at 100 MPa. The as-obtained pellets with 10 mm diameter and 0.8 mm thickness were then sintered at various temperatures from 1100 to 1200 °C, for 1 h in air. Samples with apparent densities of 94–96% of the theoretical density were obtained. The densities of the sintered pellets were measured by Archimede's method (in water) using a density balance. Fig. 6 shows the SEM micrographs of the NBT-$BT_{0.05}$ samples sintered at 1100–1200 °C. The grains size and relative density of the sintered pellets at various temperatures are shown in Table 1.

Fig. 7 shows the dielectric constants (ε_r) and dielectric losses ($\tan\delta$) as a function of temperature at frequencies ranging from 1 to 100 kHz, for unpoled NBT-$BT_{0.05}$ ceramics sintered at temperatures of 1100 (a), 1150 (b) and, 1200 °C (c). It can be seen that the dielectric constants show obvious frequency dispersion and exhibit broad dielectric peaks with a maximum at T_m of 246–299 °C temperature range. These results indicate that the as-prepared NBT-$BT_{0.05}$ ceramics are relaxors ferroelectric and the T_m is 94–41 °C lower than that of pure $Na_{0.5}Bi_{0.5}TiO_3$ (340 °C).[24,25] The permittivity decreases with increasing frequency from 1 kHz to 100 kHz. At relatively low frequency (100 Hz, shown only in Fig. 7(a)), ε_r depends on frequency strongly, showing a dielectric dispersion evidently. This strong dispersion seems to be a common feature in ferroelectric

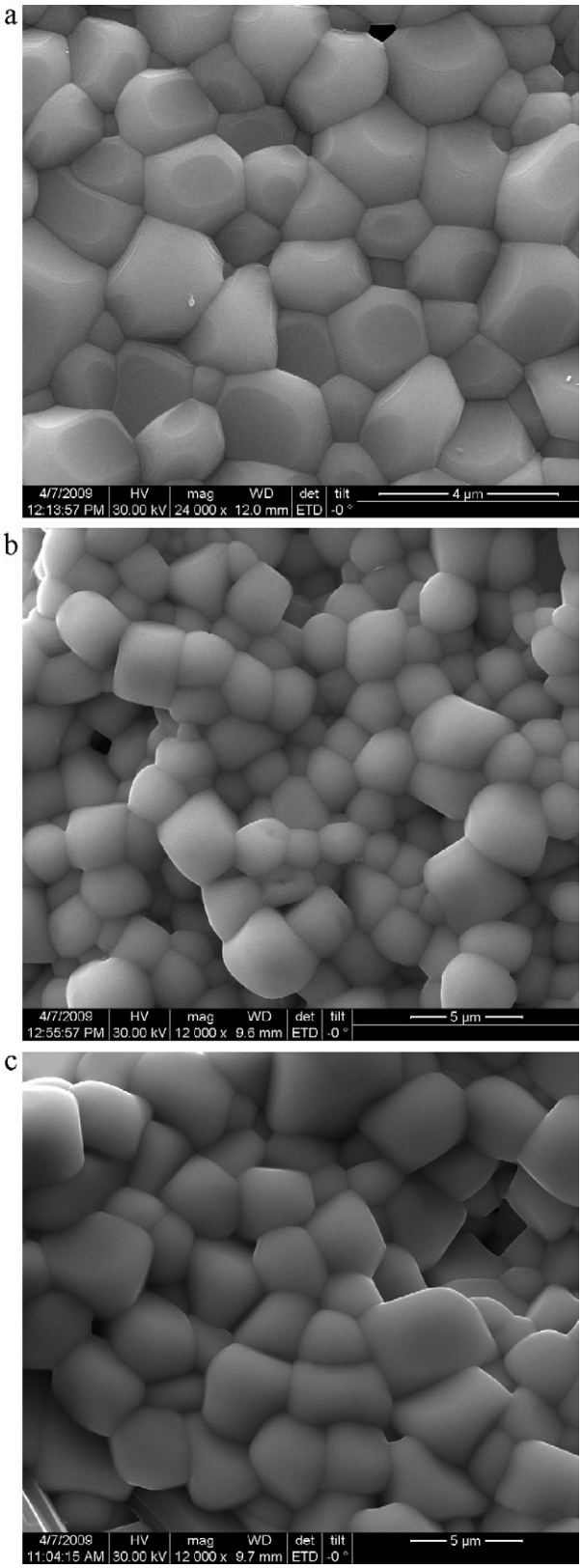

Fig. 6. SEM micrographs of NBT-$BT_{0.05}$ ceramic sintered at: (a) 1100 °C, (b) 1150 °C and (c) 1200 °C, 1 h in air.

Table 1
Structural and dielectric characteristics of unpoled NBT-$BT_{0.05}$ ceramics compared with published values for NBT-BT_x.

$T_{sintering}$ (°C)	Average grain size (μm)	Relative density $\rho/\rho_{theor.}$ (%)	Frequency, (kHz)	Temperature of maximum of dielectric constant T_m, (°C)	Dielectric constant ε_r		Dielectric loss, tan δ
					This paper	Ref.[9]	
1100	2.0	95.6	1	246	4221	4000/x = 0.05; 5000/x = 0.06 at T_m = 300 °C, and 1 kHz	0.032
			10	246	4080		0.032
			100	246	3953		0.027
1150	2.5	95.4	1	248	3940		0.016
			10	248	3845		0.014
			100	248	3786		0.006
1200	3.0	94.7	1	299	2232		0.192
			10	299	2115		0.184
			100	299	2032		0.179

materials concerned with ionic conductivity, which is referred as low-frequency dielectric dispersion.[26] When the frequency increases, the relative effect of ionic conductivity becomes small and as a result, the frequency dependence of ε_r becomes weak. In contrast, tan δ reveals a different variation with frequency and increases when frequency rises, which can be ascribed to ionic conductivity. With an increase in frequency, retardation in polarization caused from ionic conductivity is enhanced, leading to an increase in tan δ.[27,28] Permittivity decreases and the maximum dielectric temperature (T_m) increases, when the sintering temperature of the ceramics samples increases from 1100 to 1200 °C, (Fig. 7a–c and Table 1). With increasing the sintering temperature, the dielectric loss of NBT-$BT_{0.05}$ ceramics shows a minimum value at 1150 °C.

Depolarization temperature T_d, derived from the temperature of tan δ first peak of the poled specimens,[29] has a small variation with frequency and its value is –139 °C (Fig. 8). T_d is the temperature at which the phase transition from ferroelectric (rhombohedral) to anti-ferroelectric phase (tetragonal)[30,31] occurs.

Table 2
Piezoelectric and ferroelectric properties of NBT-$BT_{0.05}$ ceramics sintered at 1150 °C and poled, compared with published values for NBT-BT_x.

Properties			This paper	Ref.[9]	Ref. [12]; x = 0.08
Electromechanical coupling factors	k_p		0.091	0.27, x = 0.04; 0.28, x = 0.06	0.047
	k_{31}		−0.055		−0.029
	k_t		0.105		0.074
Frequency constants	N_p	[m/s]	2923		2890
	N_t	[m/s]	2329		2051
Piezoelectric charge coefficient	d_{31}	[pC/N]	−16.62		−8.96
	d_{33}	[pC/N]	77	118, x = 0.04; 142, x = 0.06	26
Piezoelectric voltage coefficient	g_{31}	[10^{-3} Vm/N]	−1.738		−0.869
	g_{33}	[10^{-3} Vm/N]	8.100		2.489
Dielectric loss	tan δ		0.045		0.02
Dielectric constant	ε_{33}^T		1080		1164
	ε_{33}^T		1060		1155
Elastic stiffness	C_{33}^D	[10^{10} N/m^2]	12.17		9.45
	C_{33}^D	[10^{10} N/m^2]	12.17		9.50
Elastic compliance	S_{11}^E	[10^{-12} m^2/N]	9.58		9.53
	S_{12}^E	[10^{-12} m^2/N]	−2.665		−2.51
Mechanical quality factor	Q_m		197.5		482.4
Poisson factor	σ^E		0.2782		0.2637
Sonic velocity	V_l^E	[m/s]	4334		
Acoustic impedance	Za	[10^6 kg/(m^2 s)]	24.09		
Temperature of maximum of dielectric constant	T_m	(°C)	342		
Depolarization temperature	T_d	(°C)	139		

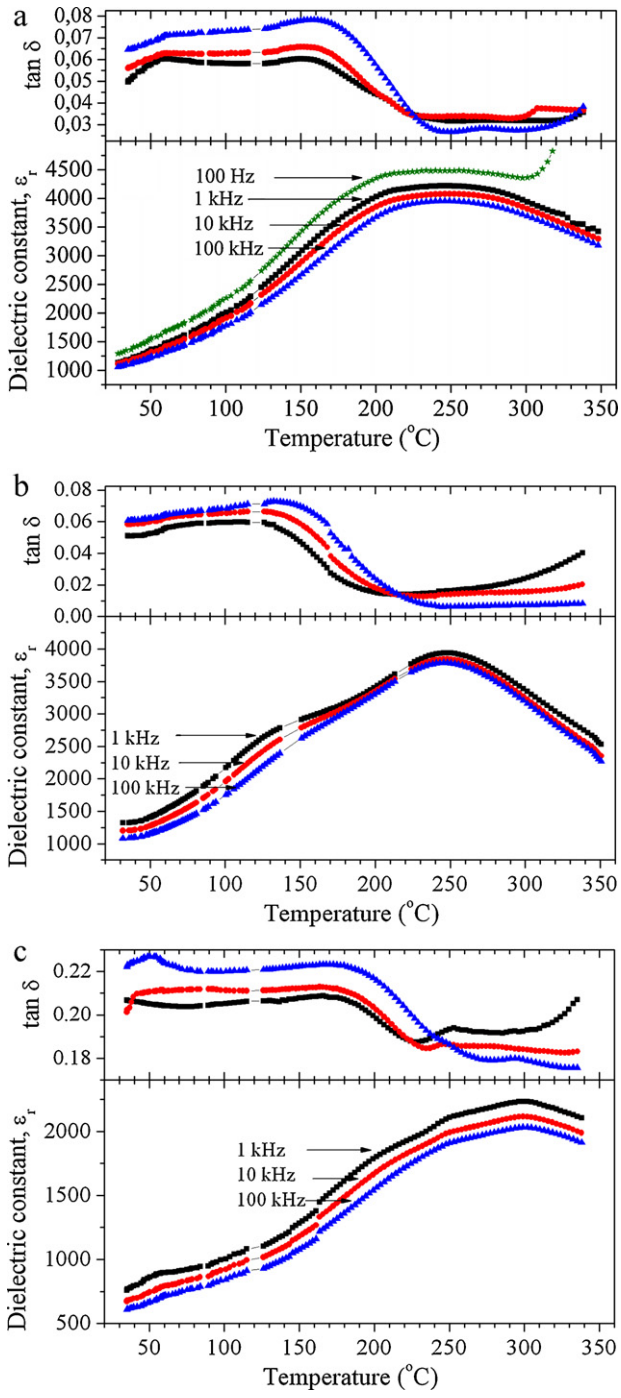

Fig. 7. Temperature and frequency dependence of dielectric constant and dielectric loss of unpoled NBT-$BT_{0.05}$ ceramic sintered at: (a) 1100 °C, (b) 1150 °C and, (c) 1200 °C.

The results of the piezoelectric characterization of the NBT-$BT_{0.05}$ ceramic sintered at 1150 °C, 2 h, at room temperature and for the resonant frequency, are shown in Table 2.

There are not many references on the characterization of NBT-$BT_{0.05}$ piezoelectric ceramic. West D. L. et al.[8] and Kim B. H. et al.,[9] which prepared NBT-$BT_{0.05}$ by an aqueous citrate-gel route and by emulsion method respectively, report similar values for dielectric constant (ε_r ~4000) and dielectric losses

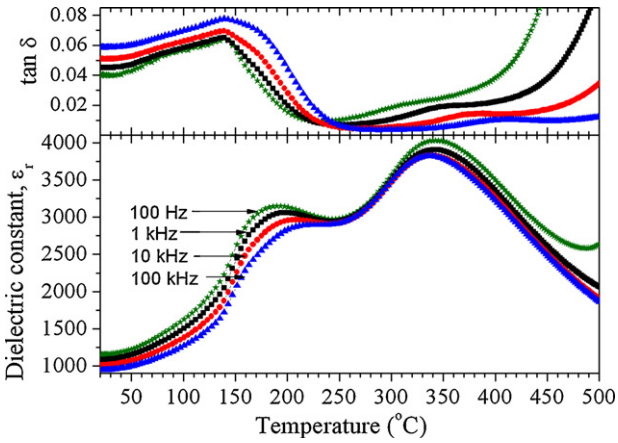

Fig. 8. Temperature and frequency dependence of dielectric constant and dielectric loss of NBT-$BT_{0.05}$ ceramic sintered at 1150 °C and poled.

(tan δ ~0.02) to that obtained by us. Chu B. J. et al.,[32] report for NBT-$BT_{0.04}$ ceramic prepared by the conventional mixed oxides method, values of 87 pC/N, 445 and 0.02 for, piezoelectric constant d_{33}, relative dielectric constant and dielectric loss, respectively. Compared with the piezoelectric properties of our NBT-$BT_{0.08}$ ceramic prepared by sol–gel,[12] this NBT–$BT_{0.05}$ ceramic shows slightly greater values for k_t, d_{33} and g_{33}, and slightly smaller values for ε_{33}, and Q_m.

4. Conclusions

Lead-free piezoelectric ceramic based on bismuth sodium titanate $(Na_{1/2}Bi_{1/2})TiO_3$ doped with 5 mol%$BaTiO_3$ was prepared by sol–gel method. X-ray diffraction analysis shows that the dried gel powder crystallizes on the rhombohedral $(Na_{0.5}Bi_{0.5})TiO_3$ lattice at 700 °C. SEM and TEM micrographs indicate that the microstructure of NBT-$BT_{0.05}$ powder consists of nano-sized grains (about 50 nm). The NBT-$BT_{0.05}$ ceramics derived from sol–gel, shown good dielectric properties. The piezoelectric properties and the high T_m temperature highlight recommend the as-obtained NBT–$BT_{0.05}$ ceramic for applications as ceramic resonator and high power applications.

Acknowledgement

The authors gratefully acknowledge the Romanian Research Ministry PNCDI II, Contract nr. 72-153/2008, for financial support.

References

1. Chen M, Xu Q, Kim BH, Ahn BK, Chen W. Effect of CeO_2 addition on structure and electrical properties of $(Na_{0.5}Bi_{0.5})_{0.93}Ba_{0.07}TiO_3$ ceramics prepared by citric method. *Mater Res Bull* 2008;**43**:1420–30.
2. Wang H, Zuo R, Ji X, Xu Z. Effects of ball milling on microstructure and electrical properties of sol–gel derived $(Na_{0.5}Bi_{0.5})_{0.94}Ba_{0.06}TiO_3$ piezoelectric ceramics. *Mater Des* 2010;**31**:4403–7.
3. Ullah A, Ahn CW, Hussain A, Kim IW. The effects of sintering temperatures on dielectric, ferroelectric and electric field-induced strain of lead-free $Bi_{0.5}(Na_{0.78}K_{0.22})_{0.5}TiO_3$ piezoelectric ceramics synthesized by the sol gel technique. *Curr Appl Phys* 2010;**10**:1367–71.

4. Takahashi H, Numamoto Y, Tani J, Matsuta K, Qiu J, Tsurekawa S. Lead-free barium titanate ceramics with large piezoelectric constant fabricated by microwave sintering. *Jpn J Appl Phys* 2006;**45**:L30–2.
5. Li HD, Feng C, Yao WL. Some effects of different additives on dielectric and piezoelectric properties of $(Na_{1/2}Bi_{1/2})TiO_3$–$BaTiO_3$ morphotropic-phase-boundary composition. *Mater Lett* 2004;**58**:1194–8.
6. Mercadelli E, Galassi C, Costa AL, Albonetti S, Sanson A. Sol–gel combustion synthesis of NBBT powders. *J Sol-Gel Sci Technol* 2008;**46**: 39–45.
7. Setasuwon P, Vaneesorn N, Kijamnajsuk S, Thanaboonsombut A. Nanocrystallization of $Na_{0.5}Bi_{0.5}TiO_3$ piezoelectric material. *Sci Technol Adv Mater* 2005;**6**:278–81.
8. West DL, Payne DA. Preparation of $0.95(Na_{1/2}Bi_{1/2})TiO_3$–$0.05BaTiO_3$ ceramics by an aqueous citrate–gel rout. *J Am Ceram Soc* 2003;**86**:192–4.
9. Kim BH, Han SJ, Kim JH, Lee JH, Ahn BK, Xu Q. Electrical properties of $(1-x)(Na_{1/2}Bi_{1/2})TiO_3$–$xBaTiO_3$ synthesized by emulsion method. *Ceram Int* 2007;**33**:447–52.
10. Pookmanee P, Rujijanagul G, Ananta S, Heimann RB, Phanichphant S. Effect of sintering temperature on microstructure of hydrothermally prepared bismuth sodium titanate ceramics. *J Eur Ceram Soc* 2004;**24**: 517–20.
11. Hao J, Wang XH, Chen RZ, Li LT. Synthesis of $Na_{0.5}Bi_{0.5}TiO_3$ nanocrystalline powders by stearic acid gel method. *Mater Chem Phys* 2005;**90**:282–5.
12. Cernea M, Andronescu E, Radu R, Fochi F, Galassi C. Sol–gel synthesis and characterization of $BaTiO_3$ doped-$(Na_{1/2}Bi_{1/2})TiO_3$ piezoelectric ceramics. *J Alloys Compd* 2010;**490**:690–4.
13. Zhao ML, Wang CL, Zhong WL, Wang JF, Chen HC. Electrical properties of $Na_{0.5}Bi_{0.5}TiO_3$ ceramic prepared by sol–gel method. *Acta Phys Sin-Chin Ed* 2003;**52**:229–33.
14. Takenaka T, Maruyama KI, Sakata K. $(Na_{1/2}Bi_{1/2})TiO_3$–$BaTiO_3$ system for lead-free piezoelectric ceramics. *Jpn J Appl Phys* 1991;**30**:2236–9.
15. Chu BJ, Chen DR, Li GR, Yin QR. Effect of A-site substitution on crystal component and dielectric properties in $Na_{0.5}Bi_{0.5}TiO_3$ ceramics. *J Eur Ceram Soc* 2002;**22**:2115–21.
16. Cao WW, Cross LE. Theoretical model for the morphotropic phase boundary in lead zirconate-lead titanate solid solution. *Phys Rev B* 1993;**47**:4825–30.
17. Jones GO, Thomas PA. *Acta Crystallogr Sec B: Struct Sci* 2002;**58**:168. Pattern: 01-070-9850.
18. Li Y, Chen W, Xu Q, Zhou J, Wang Y, Sun H. Piezoelectric and dielectric properties of CeO_2-doped $Bi_{0.5}Na_{0.44}K_{0.06}TiO_3$ lead-free ceramics. *Ceram Int* 2007;**33**:95–9.
19. Xu C, Lin D, Kwok KW. Structure electrical properties and depolarization temperature of $(Bi_{0.5}Na_{0.5})TiO_3$-$BaTiO_3$ lead-free piezoelectric ceramics. *Solid State Sci* 2008;**10**:934–40.
20. Kantha P, Pengpat K, Jarupoom P, Intatha U, Rujijanagul G, Tunkasiri T. Phase formation and electrical properties of BNLT-BZT lead-free piezoelectric ceramic system. *Curr Appl Phys* 2009;**9**:460–6.
21. Zhang MS, Scott JF. Raman Spectroscopy of $Na_{0.5}Bi_{0.5}TiO_3$. *Ferroelectr Lett* 1986;**6**:147–52.
22. Trujillo S, Kreisel J, Jiang Q, Smith JH, Thomas PA, Bouvier P, et al. The high-pressure behaviour of Ba-doped $Na_{0.5}Bi_{0.5}TiO_3$ investigated by Raman spectroscopy. *J Phys: Condens Matter* 2005;**17**:6587–97.
23. Qu Y, Shan D, Song J. Effect of A-site substitution on crystal component and dielectric properties in $Bi_{0.5}Na_{0.5}TiO_3$ ceramics. *Mater Sci Eng B* 2005;**121**:148–51.
24. Li J, Wang F, Leung CM, Or SW, Tang Y, Chen X, et al. Large strain response in acceptor- and donor-doped $Na_{0.5}Bi_{0.5}TiO_3$-based lead-free ceramics. *J Mater Sci* 2011;**46**:5702–8.
25. Zvirgzds JA, Kapostis PP, Zvirgzde JV. X-ray study of phase transitions in ferroelectric $Na_{0.5}Bi_{0.5}TiO_3$. *Ferroelectrics* 1982;**40**:75–7.
26. Yordanov SP, Ivanov I, Carapanov CP. Dielectric properties of the ferroelectric $Bi_2Ti_2O_7$ceramics. *J Phys D* 1998;**31**:800–5.
27. Wang XX, Choy CL, Tang XG, Chan HLW. Dielectric behavior and microstructure of $Na_{1/2}Bi_{1/2}TiO_3$–$K_{1/2}Bi_{1/2}TiO_3$–$BaTiO_3$ lead-free piezoelectric ceramics. *J Appl Phys* 2005;**97**:104101–10414.
28. Zhou C, Liu X, Li W, Yuan C. Dielectric and piezoelectric properties of $Na_{0.5}Bi_{0.5}TiO_3$–$K_{0.5}Bi_{0.5}TiO_3$–$BiCrO_3$ lead-free piezoelectric ceramics. *J Alloys Compd* 2009;**478**:381–5.
29. Yoshii K, Hiruma Y, Nagata H, Takenaka T. Electrical Properties and Depolarization Temperature of $(Na_{1/2}Bi_{1/2})TiO_3$–$(K_{1/2}Bi_{1/2})TiO_3$ Lead-free Piezoelectric Ceramics. *Jpn J Appl Phys* 2006;**45**:4493–6.
30. Suchanicz J, Ptak WS. On the phase transition in $Na_{0.5}Bi_{0.5}TiO_3$. *Ferroelectr Lett* 1990;**12**:71–8.
31. Suchanicz J. Behavior of $Na_{0.5}Bi_{0.5}TiO_3$ ceramic in the A.C. electric field. *Ferroelectrics* 1998;**209**:561–8.
32. Chu BJ, Cho JH, Lee YH, Kim BI, Chen DR. The potential application of NBT-based ceramics in large displacement actuation. *J Ceram Process Res* 2002;**3**:231–4.